Journal of Science and Technology in Civil Engineering, NUCE 2021. 15 (2): 26–37

SPAN LENGTH-DEPENDENT LOAD-CARRYING CAPACITY OF NORMAL CONCRETE - HPFRC BEAMS

Duy-Liem Nguyen[a,*], Tri-Thuong Ngo[b], Ngoc-Thanh Tran[c]

[a]*Faculty of Civil Engineering, Ho Chi Minh City University of Technology and Education, 01 Vo Van Ngan street, Thu Duc City, Ho Chi Minh city, Vietnam*
[b]*Faculty of Civil Engineering, Thuyloi University, 175 Tay Son street, Dong Da district, Hanoi, Vietnam*
[c]*Faculty of Civil Engineering, Ho Chi Minh City University of Transport, 02 Vo Oanh street, Binh Thanh district, Ho Chi Minh city, Vietnam*

Article history:
Received 28/12/2020, Revised 16/03/2021, Accepted 30/03/2021

Abstract

The dependence of load-carrying capacity on span length of beams, which contained a combination of normal strength concrete (NC) - High-performance fiber-reinforced concrete (HPFRC), was investigated in this study. The used HPFRC contained 1.0 vol.% long hooked blended with 0.5% short smooth fibers. Two types of span length were designed as 300 mm and 450 mm while dimensions of beam sections were identical with depth × width of 150 × 150 mm^2. Each span included five types of partial structural materials as follows: Short 1 and Long 1 had no reinforcement with full of section using HPFRC, Short 2 and Long 2 had reinforcements with a full of section using HPFRC, Short 3 and Long 3 had reinforcements with a half of section using HPFRC at beam bottom, Short 4 and Long 4 had reinforcements with a third of section using HPFRC at beam bottom, Short 5 and Long 5 had reinforcements with a half of section using HPFRC at beam top. All beams were tested under three-point bending test. The shorter beam generally exhibited the greater load-carrying capacity than the long beam using same section type. The shear failure mode was dominant in case of the span/depth ratio less than 3. The HPFRC located at bottom of beam created the more effectiveness for enhancement of load-carrying capacity and stiffness of the beam, in comparison with the HPFRC placed at top of beam. The most effective zone of beam for HPFRC strengthening was at extreme tension fiber.

Keywords: high-performance; composite beam; shear failure; bending resistance; load-carrying capacity.

https://doi.org/10.31814/stce.nuce2021-15(2)-03

1. Introduction

Traditional normal strength concrete (NC) has long been applied as one of the main construction materials. However, this material is characterized by a relative weak tensile strength accompanied by low cracking resistance. This causes the quick deterioration of civil infrastructures and attracts researchers' attention for developing new better concretes. High-performance fiber-reinforced concretes (HPFRCs) have been considered as one of promising construction materials for enhancing structural and cracking resistances. The superior properties of HPFRCs accompanied by work-hardening behaviors with multiple tiny cracks after the first crack; this phenomenon leads to high strengths in both tension and compression, high ductility and large energy absorption capacity [1–4]. Besides, the densified microstructure and fiber-bridging mechanism of HPFRC also produce its high cracking

*Corresponding author. *E-mail address:* liemnd@hcmute.edu.vn (Nguyen, D.-L.)

resistance [5–7]. The superior properties of HPFRCs are greatly expected to bring low maintenance and management cost as well as high durability of civil infrastructures. In Vietnam, the application of HPFRCs is more and more popular, e.g., the deck slab of Thang Long bridge (Hanoi), as described in Fig. 1a and towers of the extradosed bridge of Metro line 1 (Ho Chi Minh city), as described in Fig. 1b. In addition to applying for constructing structures, HPFRC may be used for rehabilitating existing structures. Some available references [8–11] provided the information on the practicable combination between HPFRC (or UHPFRC) and NC for strengthening a concrete beam. Recently, the composite beams using NC and HPFRC together were reported in the previous studies by the first author [12, 13]. On the other hand, load-carrying capacity of beams and failure modes were significantly dependent on span-length/depth ratio [14, 15], and hence, this experimental research would focus on this matter, i.e., the span length-dependent load-carrying capacity of reinforced normal concrete-HPFRC beams. The research is believed to provide useful information in application of HPFRC for rehabilitating existing flexural members.

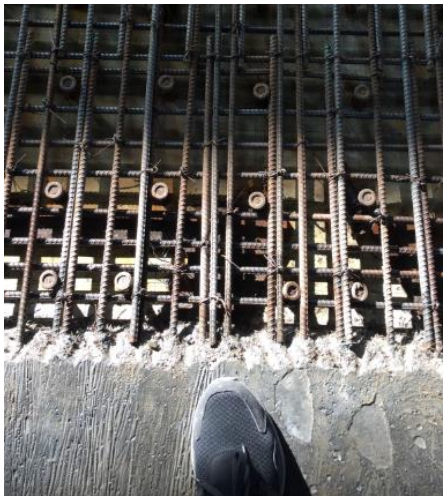

(a) HPFRC used for rehabilitating deck slab, Thang Long bridge, Hanoi

(b) HPFRC used for saddle anchor of extradosed bridge, Metro line 1, Ho Chi Minh city

Figure 1. Recent applications of HPFRCs for bridges in Vietnam

2. Influence of span-length on flexural resistances

2.1. Load versus deflection relationship

The studied flexural resistances would be evaluated including load-carrying capacity and corresponding deflection capacity. Fig. 2 performs the moment and shear distributions under three-point bending load. As presented in Fig. 2, the moment ($M = PL/4$) revealed the highest value at mid-span and shear force ($V = P/2$) was uniform along the beam, i.e., the critical zone in failure of beam might be around mid-span and/or support vicinity of beam. Regarding theory of linear elasticity, the mid-span deflection (δ) of a beam under three-point bending could be the total of deflection due to moment (δ_M) and deflection due to shear force (δ_V), as given in Eq. (1) [16].

$$\delta = \delta_M + \delta_V = \frac{PL^3}{48EI}\left[1 + \frac{2\,(1+\nu)}{\psi}\left(\frac{h}{L}\right)^2\right] \tag{1}$$

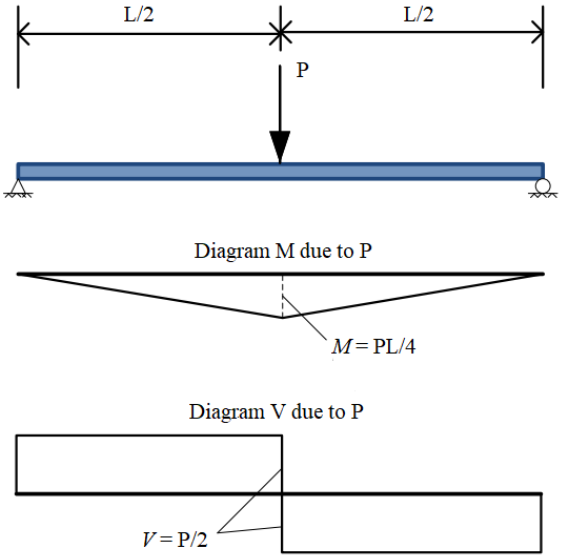

Figure 2. Moment and shear distributions under three-point bending load

where δ is the deflection at mid-span, P is the applied load, L is span-length while h is the depth of beam section, ν and ψ are the Poisson's ratio and shear coefficient of the material, respectively, E is the elastic modulus of material and I is the moment of inertia of beam.

In Eq. (1), the first and second term in bracket indicate the fraction of δ_M and δ_V, respectively. With $\nu = 0.2$ for concrete, $1/\psi = 1.5$ for the rectangular section, the short beam and long beam, characterized by $h/L = 1/2$ and $h/L = 1/3$, respectively, would lead to their mid-span deflections as given in Eqs. (2) and (3), respectively. As shown in these equations, shear force would increase the mid-span deflection 0.9 times in the short beam and 0.4 times in the long beam. In a very long beam, $h/L = 1/10$ for example, δ_V becomes rather small in comparison with δ_M, about 4% only. This means the failure of the long beam would be dominated by the bending moment.

$$\delta_{h/L=1/2} = \delta_M + \delta_V = \frac{1.9PL^3}{48EI} \tag{2}$$

$$\delta_{h/L=1/3} = \delta_M + \delta_V = \frac{1.4PL^3}{48EI} \tag{3}$$

2.2. *Failure modes in beam according to cracking behavior*

Failure modes in a RC beams can generally be classified into two main forms: flexural failure with its identification of vertical crack and shear failure with its identification of diagonal crack. The failure of the RC beam happens as the internal moment or shear force exceeds moment resistance or shear resistance, respectively. Considering a RC beam subjected to loading, the failure of beam may be influenced by the following factors: shear span to effective depth ratio, longitudinal reinforcing bar ratio, aggregate type, concrete strength, loading type and support conditions.

Fig. 3 displays main failure modes of a RC beam, the descriptions of these failures accompanied with their cracking behaviors were detailed as follows [17]:

a. Flexure failure

This failure of structure is caused by the crushing of the concrete in compression zone after yielding of the reinforcing bar, it often occurs at bottom in mid-span zone due to moment. The crack initiates from the bottom with vertical direction toward the neutral axis of beam, as illustrated in Fig. 3(a).

b. Flexure-shear failure

This failure usually occurs in RC beam with low amount of stirrups and longitudinal reinforcement. The crack initiates at beam bottom with vertical direction owing to flexural tensile stress then propagates in a diagonal direction over the whole cross section until collapse, as illustrated in Fig. 3(b).

c. Shear compression failure

This failure often occurs in RC beam with low amount of web reinforcement but adequate longitudinal reinforcement. Shear crack may easily start from former flexural cracks but it does not propagate through the compression zone. The failure is governed by concrete crushing in compression zone above the tip of the shear crack and named shear compression failure, as illustrated in Fig. 3(c).

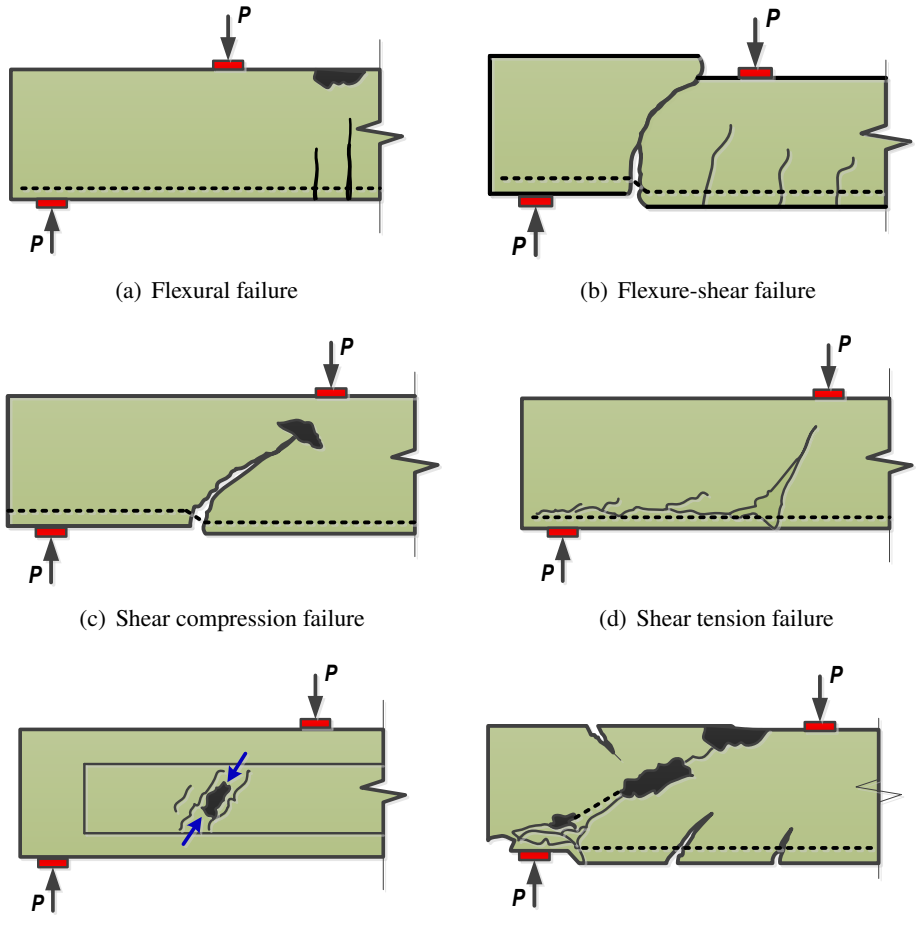

(a) Flexural failure (b) Flexure-shear failure

(c) Shear compression failure (d) Shear tension failure

(e) Web crushing failure (f) Arch rib failure

Figure 3. Failure modes of the RC beam

d. Shear tension failure

This failure occurs in RC beam with a debond between main longitudinal reinforcement and surrounding concrete. The debond may be caused by an inadequate anchorage of the longitudinal bars or concrete cover. Cracks appear along the longitudinal reinforcement till they join with a flexure-shear crack causing shear tension failure, as shown in Fig. 3(d).

e. Web crushing failure

This failure often appears in thin-webbed RC beams with large amount of transverse reinforcement, the concrete crushing occurs in the diagonal struts, as shown in Fig. 3(e).

f. Arch rib failure

This failure usually occurs in deep beams or short beams in which the direct force transferring from the load location to the bearings is dominant, as illustrated in Fig. 3(f).

In fact, some failure modes can totally be as a combination of more than one of failure modes mentioned above, for example, shear tension failure and shear compression failure.

3. Experiment

3.1. Materials and beam preparation

Fig. 4 presents the experimental outline with two ratios of span length/depth of beam: 2 for shorter beams and 3 for longer beams; each ratio of span length/depth includes five section types as detailed in Fig. 4. All beams were designed with a constant depth and width of 150 mm, full length of the short beams and long beams were 400 mm (span-length of 300 mm) and 600 mm (span-length of 450 mm), respectively. Table 1 displays the composition of plain HPFRC and normal concrete (NC). The compressive strengths, using cylindrical-shaped specimens with 150 mm in diameter and 300 mm in height, of HPFRC and NC were 79.6 MPa and 20.2 MPa, respectively. The direct tensile strength of HPFRC experimentally was 9.81 MPa [13] whereas that of NC was estimated to be 1.48 MPa according to ACI 318 [18]. Beam Type 1 had no reinforcing bar while other types, from beam Type 2 to beam Type 5, were designed using 2 bars in tensile zone with diameter of 12 mm (A_s = 2.26 cm^2, cover t_0 = 25 mm) and 2 bars in compressive zone with diameter of 6 mm ($A_s^{'}$ = 0.57 cm^2,

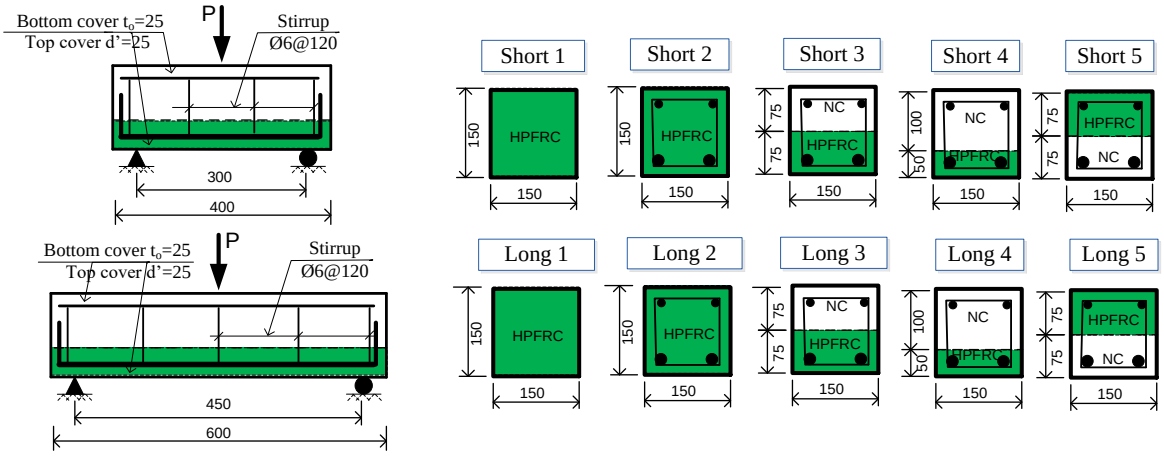

Figure 4. Experimental outline

cover d' = 25 mm). The yield strength of steel bars was f_y = 400 MPa while that of stirrup was f'_y = 240 MPa. Stirrup spacing was 120 mm in both of short and long beams. NC and HPFRC were mixed immediately after each other. It was noticed that the tested beams were designed regarding intended failures, not for full-scale and/or scale-down test, therefore, these tests are also needed in further investigations.

The fiber size and aspect ratio were reported to importantly affect the tensile behaviors of HPFRC [19, 20]. The combination between short and long fibers could create the synergy effect on enhancing mechanical properties of HPFRC [13, 21, 22]. Hence, the HPFRC placed in beams were used hybrid fibers: long hooked fibers with volume fraction of 1.0% and short smooth fibers with volume fraction of 0.5%. Features of the hybrid fibers were shown in Table 2 and their photos were presented in Fig. 5. The aspect ratios of long hooked and short smooth fibers were 35/0.5 and 13/0.2, respectively. All specimens/beams after pouring were located in an experimental room for 2 days prior to demolding. The specimens/beams after demolding were cured in water at 25±5 °C for 28 days and they would be tested at 30-day age in dry condition.

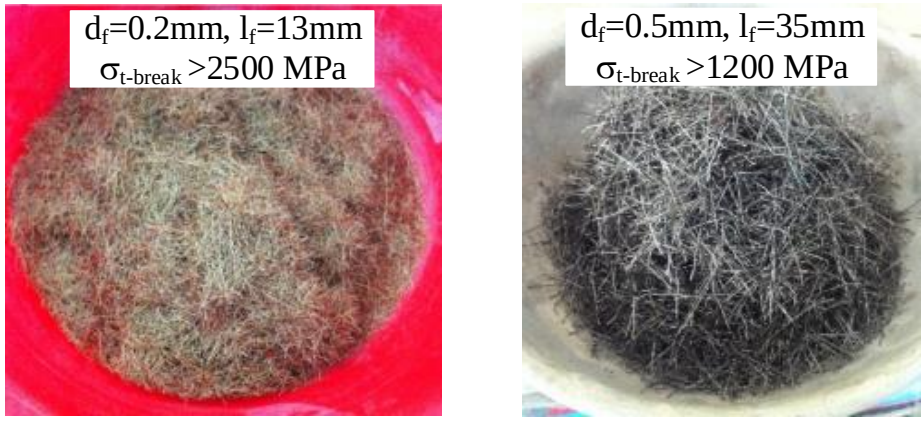

(a) Short smooth fibers, 0.5 vol.% (b) Long hooked fibers, 1.0 vol.%

Figure 5. Photos of hybrid fibers mixed in HPFRC

Table 1. Composition and compressive strength of HPFRC and NC used

Mixture type	Cement (Insee, PC40)	Silica Fume	Silica sand	Fly ash	Superplas -ticizer	Coarse aggregate	Water	Compressive strength (MPa)
HPFRC	0.80	0.07	1.00	0.20	0.04		0.26	79.6
NC	1.00	-	2.23	-	-	4.62	0.63	20.2

Direct tensile strength of HPFRC was 9.81 MPa [13]

3.2. Test setup

All beams were tested under three-point bending load using a universal test machine with 1 mm/min crosshead speed in displacement control mode. The frequency of data acquisition under tests was 1 Hz. During experiment, the load history and its corresponding deflection of the tested beams

Table 2. Features of the hybrid fibers used

Notation	Diameter (mm)	Length (mm)	Aspect ratio (L/D)	Tensile strength (MPa)
Long Hooked	0.5	35	70	> 1200
Short Smooth	0.2	13	65	> 2500

were recorded in the test machine, these data were then analyzed and evaluated. Fig. 6 illustrates the test set-up under three-point bending load.

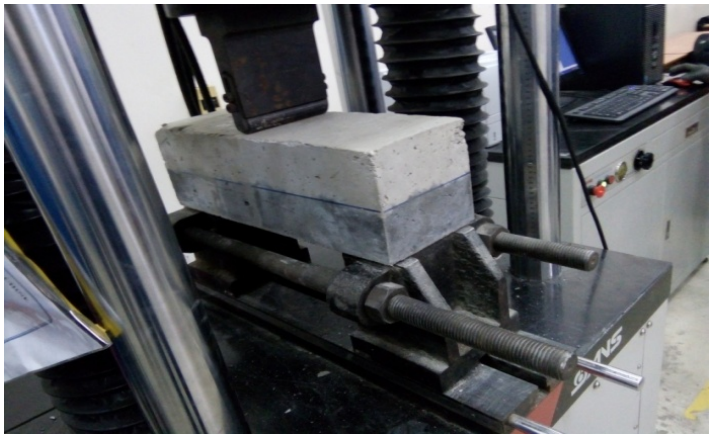

Figure 6. Test set-up under three-point bending load

4. Experiment result and discussion

4.1. Load versus deflection behaviors of the studied beams

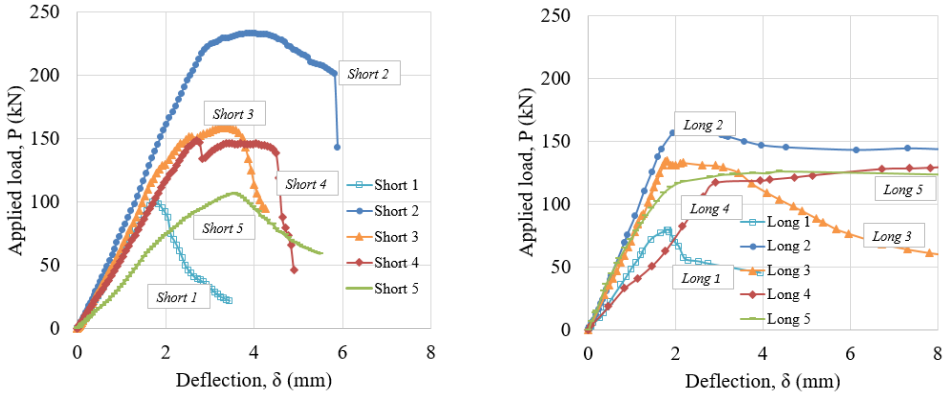

(a) Behaviors of the short beams

(b) Behaviors of the long beams

Figure 7. Load versus deflection behavior of the studied beams

Figs. 7(a) and 7(b) display the load versus deflection responses of the short and long beams, respectively. Generally, the short beams generated the higher load-carrying capacity but lower deflection capacity. These results were entirely acceptable because the shorter span-length would produce the lower internal moment and lower deflection with same applied load, as presented in Section 2. Table 3 provides the load-carrying capacity (maximum load, P_{max}) and the angle (θ) and mode of failure cracks of the tested beams.

Table 3. Load-carrying capacity and failure mode of the beams

Beam name	P_{max} (kN)	θ (degree)	Failure mode	Beam name	P_{max} (kN)	θ (degree)	Failure mode
Short 1	100.39	85	flexure	Long 1	79.48	85	flexure
Short 2	233.57	65	flexure-shear	Long 2	160.67	60	flexure-shear
Short 3	158.49	50	arch rib	Long 3	147.47	55	arch rib
Short 4	148.90	45-75	arch rib	Long 4	134.93	80	flexure-shear
Short 5	106.59	45	shear comp.	Long 5	126.28	35-75	shear comp.

The significances in the increases of P_{max} between short and long beams were shown in Fig. 8. Comparatively, the increases of load-carrying capacities were from 1.07 times (Short 3/Long 3) to 1.45 times (Short 2/Long 2), except for Short 5/Long 5 with a decrease of 0.84 times. This special case was thought due to a mistake at Short 5 or Long 5 and should be confirmed again in further study. Although the long beam was slender than the short, its shear effect was still important, e.g., the deflection due to shear up to 40% the deflection due to moment according to Eq. (3). This caused both short and long beams to demonstrate generally same failure modes.

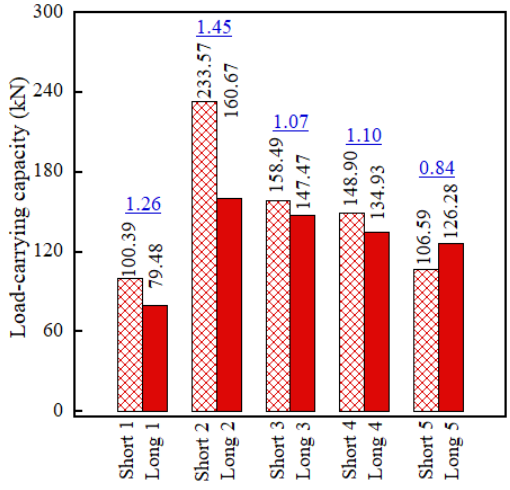

Figure 8. Load-carrying capacities of the studied beams

As the thickness of HPFRC layer decreased (Type 2 > Type 3 > Type 4), the load-carrying capacity of the beams was reduced. This trend was completely suitable because the strength of HPFRC was greater than that of NC, and a lower HPFRC thickness placed at beam bottom would cause a lower mechanical resistance of beam. Moreover, although beam Type 3 and Type 5 contained a half of HPFRC on beam section, HPFRC placed in tensile zone (beam Type 3) was observed to be more effective than HPFRC placed in compressive zone (beam Type 5). This phenomenon could be attributed that the tensile resistance and compressive resistance of beam Type 3 was more balanced. On the contrary, in beam Type 5, the tensile resistance of beam may be much weaker than compressive resistance and this led to the easier failure in tensile zone. Compared to Type 4, despite the fact that Type 3 with its thicker HPFRC produced the higher load-carrying capacity, its efficacy in using HPFRC was observed to be lower. In detail, as the HPFRC thickness increased 1.67 times (from 50 mm of Type 4 to 75 mm of Type

3), the load-carrying capacity increased only 1.06 times (from 148.90 kN of Short 4 to 158.49 kN of Short 3), and 1.09 times (from 134.93 kN of Long 4 to 147.47 kN of Long 3). This indicated that the HPFRC could be effectively used to rehabilitate existing structures with its amount enough at the extreme tension fiber.

4.2. Cracking behaviors of the studied beams

Fig. 9 displays the cracking behaviors of the studied beams. As summarized in Table 3, the beam Type 1 with no reinforcing bar revealed the flexure failure mode while others exhibited the flexure-shear, arch rib or shear compression failure, although some cases were not clear. For beam Type 2-Type5, the main crack did not appear at the mid-span but propagated towards the location of applied load at mid-span, as shown in Fig. 9.

4.3. Flexural strength in relationship with compressive strength of HPFRC

The flexural strength (f_{MOR}) of HPFRC under the three-point bending loading can be computed from $P_{\max}$ using Eq. (4). Based on experiments, the f_{MOR} of the short and long beams (Type 1) were 13.39 MPa and 15.90 MPa, respectively. Adopting ACI 318 [18] for NC, the flexural strength could be proportional to the square root of compressive strength, as given in Eq. (5). This relationship could also be considered for HPFRCs [23, 24] and used in this study, as given by Eq. (6). The coefficients α of the short and long beams were 1.50 and 1.78, respectively. These values were much higher than that of NC (equal to 0.65), this could be explained that the tensile resistance of HPFRC was significantly improved owing to fibers embedded in HPFRC, the fibers may generate deflection-hardening by crack-bridging mechanism. The comparative coefficients could be used to predict each other.

$$f_{MOR} = 1.5\frac{P_{\max}L}{bh^2} \tag{4}$$

$$f_r = 0.65\sqrt{f_c'} \tag{5}$$

$$f_{MOR} = \alpha\sqrt{f'_{c-HPFRC}} \tag{6}$$

where $f_c^{'}$ and $f'_{c-HPFRC}$ are the compressive strength using a cylinder specimen of 150×300 mm. L is span-length while b and h are the width and depth of beam section, respectively.

4.4. Comparative stiffnesses of the tested beams

The term of "stiffness" in this study was defined as the slope before crack of load versus deflection response curve of the tested beam, which was presented in Fig. 7. The comparison was performed for two couples: Type 1 – Type 2 with different reinforcement and Type 3 - Type 5 with different location of HPFRC layer. Table 4 provides the stiffness values of two couples: Type 2 with reinforcement bar was stiffer than Type 1 with no reinforcement bar, Type 3 with location of HPFRC layer at bottom was stiffer than Type 5 with location of HPFRC layer at top. As shown in Table 4, the stiffness of beam seemed to be dependent upon not only moment of inertia but also span-length of beam. The short beams generally exhibited the higher stiffness in comparison to the long beams with same type of section. These results were entirely appropriate since the longer beam would generate the larger deflection with an identical load, regarding Eq. (1). Only the couple of Short 1 – Long 1 showed the contrary tendency, this special case might be due to a mistake at Short 1 or Long 1 and required further investigation to confirm.

(a) Short 1 with full of HPFRC and no reinforcing bar

(b) Long 1 with full of HPFRC and no reinforcing bar

(c) Short 2 with full of HPFRC

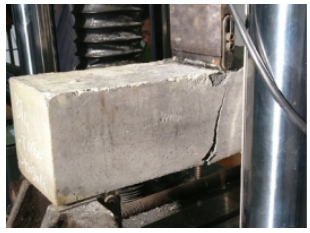

(d) Long 2 with full of HPFRC

(e) Short 3 with one-half using HPFRC at bottom

(f) Long 3 with one-half using HPFRC at bottom

(g) Short 4 with one-third using HPFRC at bottom

(h) Long 4 with one-third using HPFRC at bottom

(i) Short 5 with one-half using HPFRC at top

(j) Long 5 with one-half using HPFRC at top

Figure 9. Cracking behaviors of the studied beams

Table 4. Stiffness of the beams

Short beam	Stiffness (kN/mm)	Long beam	Stiffness (kN/mm)	Ratio short to long
Short 1	49.91	Long 1	59.66	0.84
Short 2	81.28	Long 2	68.32	1.19
Short 3	76.24	Long 3	67.81	1.12
Short 5	72.77	Long 5	37.78	1.93

5. Conclusions

The observations and conclusions can be drawn from the experimental tests as follows:

- The span length-dependent load-carrying capacity of normal reinforced concrete-HPFRC beams was clearly observed that the shorter beam would produce the greater load-carrying capacity under three-point bending, regardless of beam type.

- The shear failure mode was observed to be dominant in case of the ratio span length to depth less than 3, excepted that the HPFRC beams with no reinforcing bar revealed the flexural failure mode.

- Compared to normal concrete, the scale coefficients of flexural strength regarding square root of the compressive strength of HPFRC were notably high. The cause was thought due to fibers embedded in HPFRC with crack-bridging mechanism. Besides, the coefficients of flexural strength of HPFRC explored from the short and long beams could be used to predict each other.

- Compared to the HPFRC layer located at top of beam, the HPFRC layer located at bottom of beam created the more effectiveness for enhancing load-carrying capacity and stiffness of the beam. The most effective zone of beam for HPFRC strengthening was extreme tension fiber. The stiffness of beam seemed to be dependent upon not only moment of inertia but also span-length of beam.

Acknowledgements

This research was funded by the Vietnam National Foundation for Science and Technology Development (NAFOSTED) under grant number 107.01-2017.322. The authors are grateful for the financial support. The opinions expressed in this paper are those of the authors and do not necessarily reflect the views of the sponsors.

References

[1] Wille, K., Kim, D. J., Naaman, A. E. (2011). Strain-hardening UHP-FRC with low fiber contents. *Materials and Structures*, 44(3):583–598.

[2] Nguyen, D. L., Vu, T. B. N., Do, X. S., Tran, M. P. (2019). Using carbon black and ground granulated blast furnace slag for improvement of self-sensing capacity of high performance fiber-reinforced concretes. *Journal of Science and Technology in Civil Engineering (STCE) – NUCE*, 13(4V):151–158.

[3] Naaman, A. E., Reinhardt, H.-W. (2006). Proposed classification of HPFRC composites based on their tensile response. *Materials and Structures*, 39(5):547–555.

[4] Nguyen, D. L., Ryu, G. S., Koh, K. T., Kim, D. J. (2014). Size and geometry dependent tensile behavior of ultra-high-performance fiber-reinforced concrete. *Composites Part B: Engineering*, 58:279–292.

[5] Hoan, P. T., Thuong, N. T. (2019). Shear resistance of ultra-high-performance concrete reinforced with hybrid steel fiber subjected to impact loading. *Journal of Science and Technology in Civil Engineering (STCE)-NUCE*, 13(1):12–20.

[6] Tran, N. T., Tran, T. K., Jeon, J. K., Park, J. K., Kim, D. J. (2016). Fracture energy of ultra-high-performance fiber-reinforced concrete at high strain rates. *Cement and Concrete Research*, 79:169–184.

[7] Ngo, T. T., Park, J. K., Kim, D. J. (2019). Loading rate effect on crack velocity in ultra-high-performance fiber-reinforced concrete. *Construction and Building Materials*, 197:548–558.

[8] Bahraq, A. A., Al-Osta, M. A., Ahmad, S., Al-Zahrani, M. M., Al-Dulaijan, S. O., Rahman, M. K. (2019). Experimental and numerical investigation of shear behavior of RC beams strengthened by ultra-high performance concrete. *International Journal of Concrete Structures and Materials*, 13(1):1–19.

[9] Hussein, L., Amleh, L. (2015). Structural behavior of ultra-high performance fiber reinforced concrete-normal strength concrete or high strength concrete composite members. *Construction and Building Materials*, 93:1105–1116.

[10] Noshiravani, T., Brühwiler, E. (2013). Experimental investigation on reinforced ultra-high-performance fiber-reinforced concrete composite beams subjected to combined bending and shear. *ACI Structural Journal*, 110(ARTICLE):251–261.

[11] Martinola, G., Meda, A., Plizzari, G. A., Rinaldi, Z. (2010). Strengthening and repair of RC beams with fiber reinforced concrete. *Cement and concrete composites*, 32(9):731–739.

[12] Nguyen, D.-L., Do, V.-T., Tran, M.-P., Mai, L. (2020). Investigation on shear resistances of short beams using HPFRC composited normal concrete. In *CIGOS 2019, Innovation for Sustainable Infrastructure*, Springer, 349–354.

[13] Nguyen, D.-L., Thai, D.-K., Nguyen, H. T., Nguyen, T.-Q., Le-Trung, K. (2021). Responses of composite beams with high-performance fiber-reinforced concrete. *Construction and Building Materials*, 270: 121814.

[14] Garoushi, S., Lassila, L. V. J., Vallittu, P. K. (2012). The effect of span length of flexural testing on properties of short fiber reinforced composite. *Journal of Materials Science: Materials in Medicine*, 23 (2):325–328.

[15] Mehndiratta, A., Bandyopadhyaya, S., Kumar, V., Kumar, D. (2018). Experimental investigation of span length for flexural test of fiber reinforced polymer composite laminates. *Journal of Materials Research and Technology*, 7(1):89–95.

[16] Nguyen, D.-L., Thai, D.-K., Kim, D.-J. (2017). Direct tension-dependent flexural behavior of ultra-high-performance fiber-reinforced concretes. *The Journal of Strain Analysis for Engineering Design*, 52(2): 121–134.

[17] Sharma, R. (2014). Review on Shear Behaviour of Reinforced Concrete Beam without Transverse Reinforcement. *International Journal of Engineering Research and Applications*, 4(4):116–121.

[18] ACI 318-14. *Building code requirements for structural concrete*.

[19] Nguyen, D.-L., Nguyen, T.-Q. et al. (2020). Influence of fiber size on mechanical properties of strain-hardening fiber-reinforced concrete. *Journal of Science and Technology in Civil Engineering (STCE)-NUCE*, 14(3):84–95.

[20] Choi, W.-C., Jung, K.-Y., Jang, S.-J., Yun, H.-D. (2019). The influence of steel fiber tensile strengths and aspect ratios on the fracture properties of high-strength concrete. *Materials*, 12(13):2105.

[21] Tran, N. T., Kim, D. J. (2017). Synergistic response of blending fibers in ultra-high-performance concrete under high rate tensile loads. *Cement and Concrete Composites*, 78:132–145.

[22] Park, S. H., Kim, D. J., Ryu, G. S., Koh, K. T. (2012). Tensile behavior of ultra high performance hybrid fiber reinforced concrete. *Cement and Concrete Composites*, 34(2):172–184.

[23] Thomas, J., Ramaswamy, A. (2007). Mechanical properties of steel fiber-reinforced concrete. *Journal of Materials in Civil Engineering*, 19(5):385–392.

[24] Faisal, F. W., Ashour, S. A. (1992). Mechanical properties of high-strength fiber reinforced concrete. *ACI Material Journal*, 89(5):449–455.